**Cell Stem Cell, Volume *29***

## Supplemental Information

# Multilayer omics analysis reveals a non-classical retinoic acid signaling axis that regulates hematopoietic stem cell identity

**Katharina Schönberger, Nadine Obier, Mari Carmen Romero-Mulero, Pierre Cauchy, Julian Mess, Polina V. Pavlovich, Yu Wei Zhang, Michael Mitterer, Jasmin Rettkowski, Maria-Eleni Lalioti, Karin Jäcklein, Jonathan D. Curtis, Betty Féret, Pia Sommerkamp, Claudia Morganti, Keisuke Ito, Norbert B. Ghyselinck, Eirini Trompouki, Joerg M. Buescher, Erika L. Pearce, and Nina Cabezas-Wallscheid**

# Supplemental Figure 1

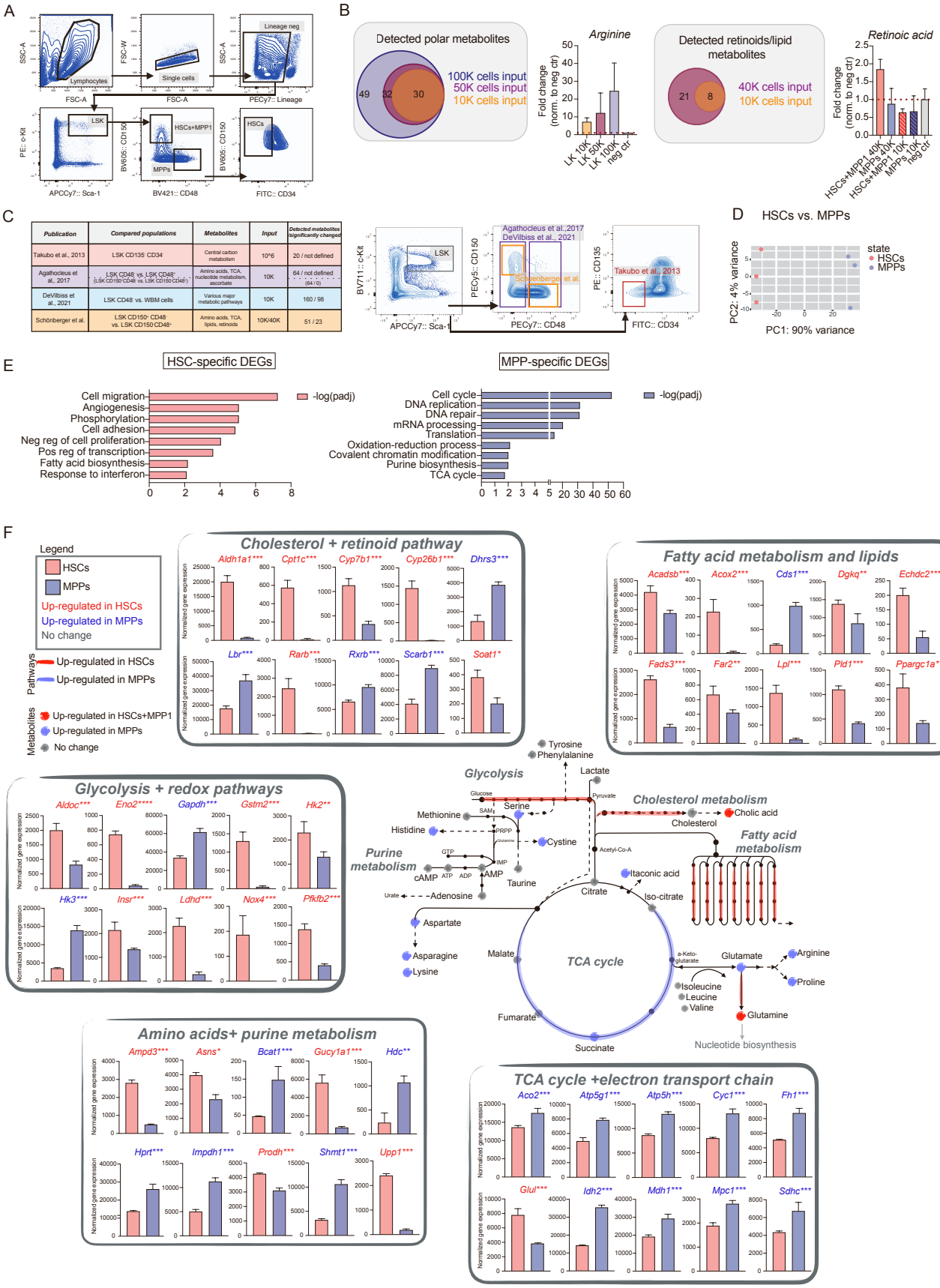

# Supplemental Figure 1

G

| Metabolic pathway | Motif | NES | PWM |
|---|---|---|---|
| Amino acids | ATF4 | 7.6 | |
| Glycolysis | HIF | 5.8 | |
| ROS | EGR | 4.7 | |
| TCA cycle | ESRR | 10.2 | |
| Fatty acids | GLI1 | 4.9 | |
| Retinoids | IRF | 5.3 | |
| Nucleotides | ESRR | 5.9 | |

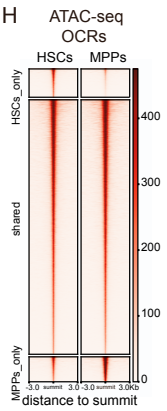


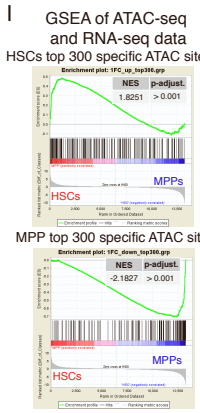


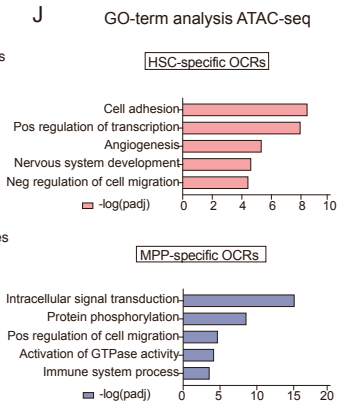


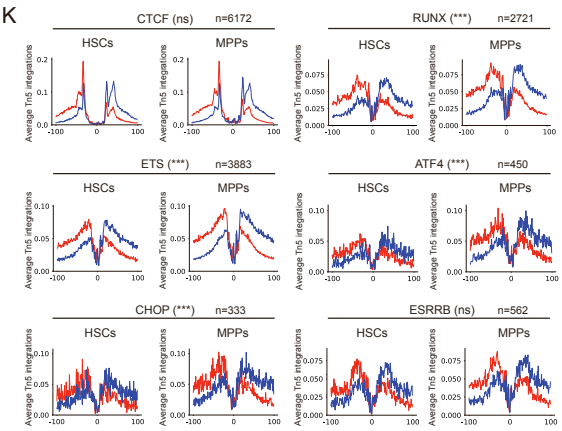


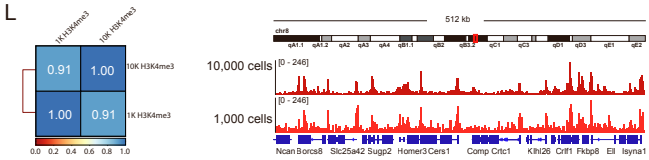


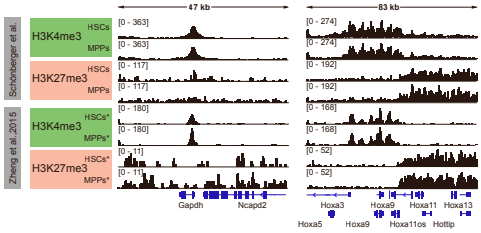


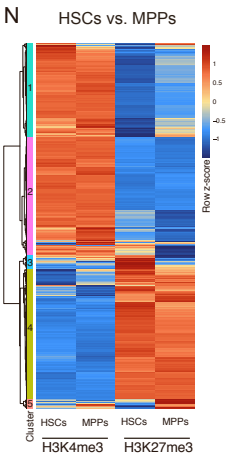


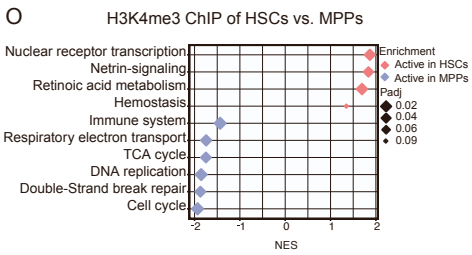


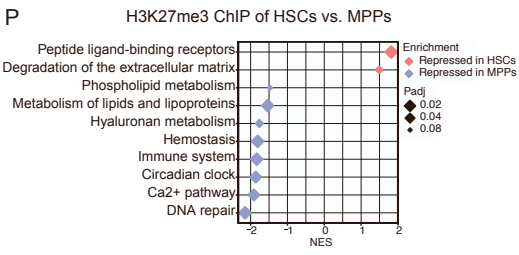


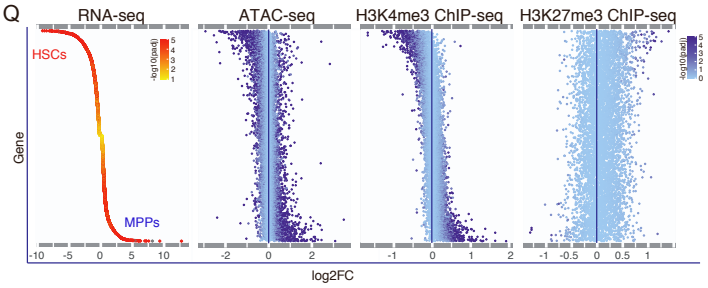


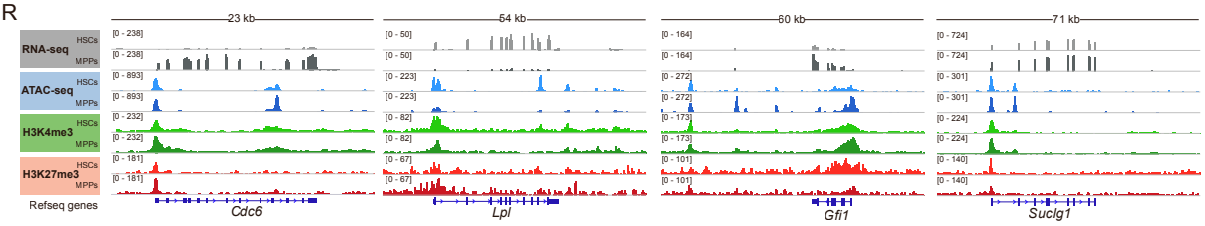

# Supplemental Figure 1

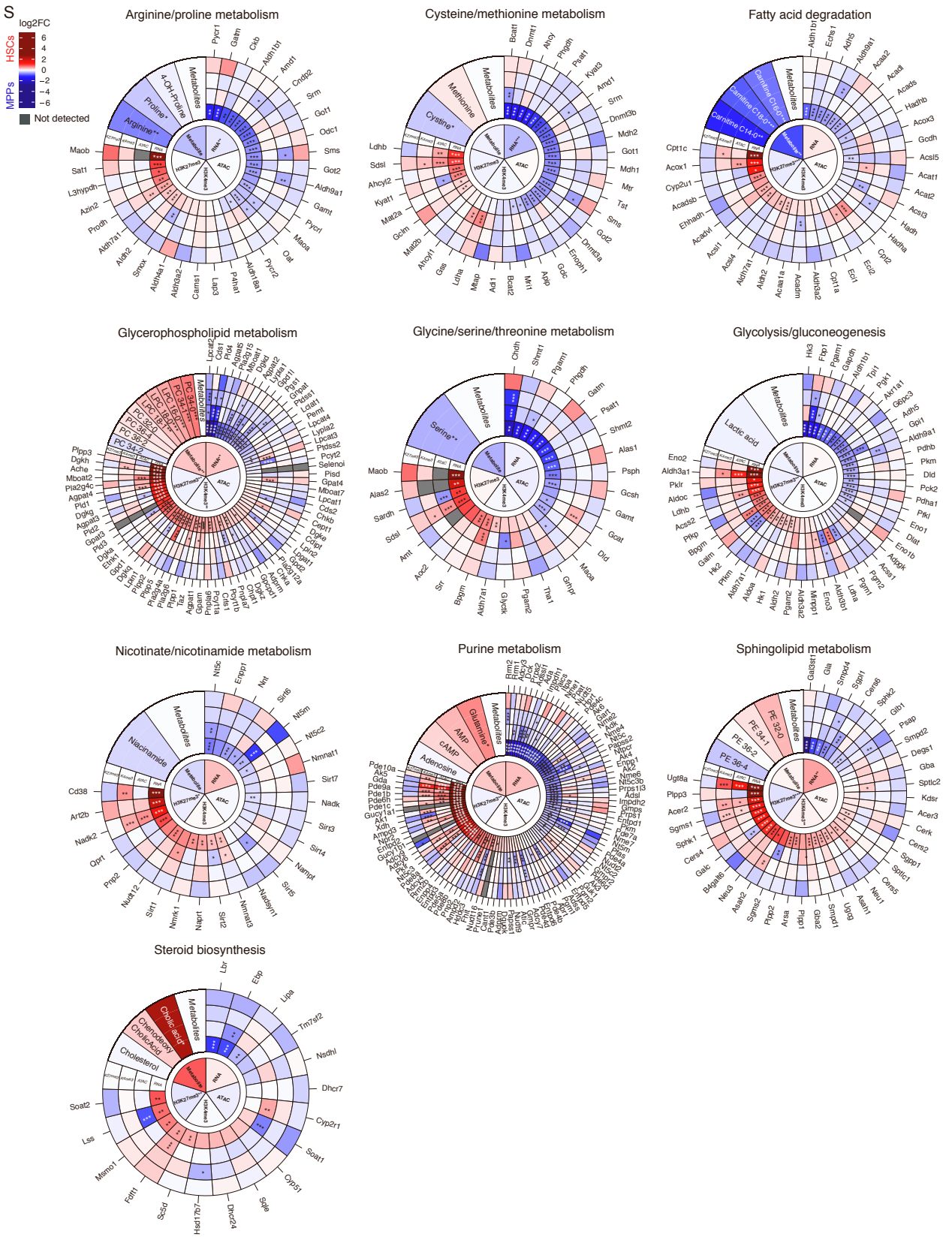

**Supplemental Figure 1 (related to Figure 1)**

**Metabolic and epigenetic landscape of HSCs and downstream progenitors**

(A) Representative gating scheme for flow cytometric cell sorting.

(B) Summary of titration experiments performed to establish targeted metabolomics methods. Correlation between cellular input and number of detected metabolites. Exemplary metabolites shown. Red dotted line indicates background level detected in negative controls.

(C) Table summarizing and comparing targeted metabolomics approaches performed on HSCs.

(D) Principle component analysis (PCA) of RNA-seq data from HSCs and MPPs. Based on top 5,000 variable genes. n=3.

(E) DAVID GO-term analysis using "Biological Processes″ based on the top 3,000 up- and down-regulated DEGs (padj.<0.1) in HSCs or MPPs.

(F) Schematic integration of targeted metabolomics results on HSCs+MPP1 and MPPs. Normalized expression counts (RNA-seq data from HSCs and MPPs; DESeq2) of selected metabolic genes are shown in bar diagrams. Metabolite names are shown in red when up-regulated in HSCs+MPP1 and in blue when up- regulated in MPPs. Significances calculated as adjusted p-values by DESeq2 *padj. <0.1; **p <0.05; ***p <0.01.
Schematic view of findings. Expression data of enzymes (RNA-seq; padj.<0.1) are shown as colored lines, red representing up-regulated in HSCs, and blue up-regulated in MPPs. Dots represent metabolites up in HSCs+MPP1 (red) or MPPs (blue).

(G) Motif enrichment analysis on DEGs between HSCs and MPPs for main metabolic processes using *i-cis target* tool. NES, Normalized enrichment score; PWM, position weight matrix.

(H) Heatmap showing clustering of ATAC-seq on HSCs and MPPs. OCRs unique to HSCs, unique to MPPs or shared are shown.

(I) GSEA of the top 300 ATAC-specific OCRs in log2FC ranked HSCs vs. MPPs RNA-seq dataset. n=3.

(J) DAVID GO-term analysis using "Biological Processes" based on genes annotated to OCRs specific to HSCs or MPPs.

(K) Digital footprinting analysis metabolic and hematopoietic TF motifs on ATAC-seq data from HSCs and MPPs. Motif occupancy on forward and reverse strand (red, blue). Significance indicated by paired student's t-test. *p <0.05; **p <0.01; ***p <0.001. ns- not significant.

(L) Titration experiment for ChIP-seq establishment on 1,000 compared to 10,000 LSK cells for H3K4me3 showing Pearson's correlation and gene tracks.

(M) Comparison of H3K4me3 and H3K27me3 data set on HSCs and MPPs with a publicly available data set (Zheng et al., 2015).*HSCs: LSK $Flk2^{-}CD34^{-}$, *MPPs: LSK $Flk2^{+}CD34^{+}$.

(N) Heatmap showing global clustering of H3K4me3 and H3K27me3 ChIP-seq row z- scores at gene transcription start site (TSS) in HSCs and MPPs. n=2-3.

(O) GSEA of selected Reactome pathways on H3K4me3 ChIP-seq in HSCs or MPPs

(P) GSEA of selected Reactome pathways on H3K27me3 ChIP-seq in HSCs or MPPs.

(Q) Swarm plots showing correlation between RNA-seq (DEGs in MPPs versus HSCs, padj.<0.1) ATAC-seq, H3K4me3 and H3K27me3 ChIP-seq data (no threshold). Pearson's correlation coefficient between transcriptome and OCRs (0.5, moderate), H3K4me3 (0.72, strong) and H3K27me3 (-0.16, very weak).

(R) Gene tracks showing exemplified genes with corresponding RNA-seq ATAC-seq, H3K4me3 and H3K27me3 ChIP-seq coverage.

(S) MTE-plots integrating metabolomics, RNA-seq, ATAC-seq, H3K4me3 and H3K27me3 ChIP-seq data on selected KEGG-pathways. Depicted is log2FC between HSCs(+MPP1) and MPPs, red indicates up-regulated in HSCs, blue up-regulated in MPPs. Significances calculated by unpaired student's t-test (metabolomics data set; *p <0.05; **p <0.01; ***p <0.001) or by DESeq2 p-adjusted value (RNA-seq, ATAC-seq, ChIP-seq data sets; *p <0.1; **p <0.05; ***p <0.01). Inner circles indicate the average tendencies of the entire KEGG pathway per data set, outer circles show individual genes/metabolites.

For all panels, n indicates number of biological replicates.

# Supplemental Figure 2

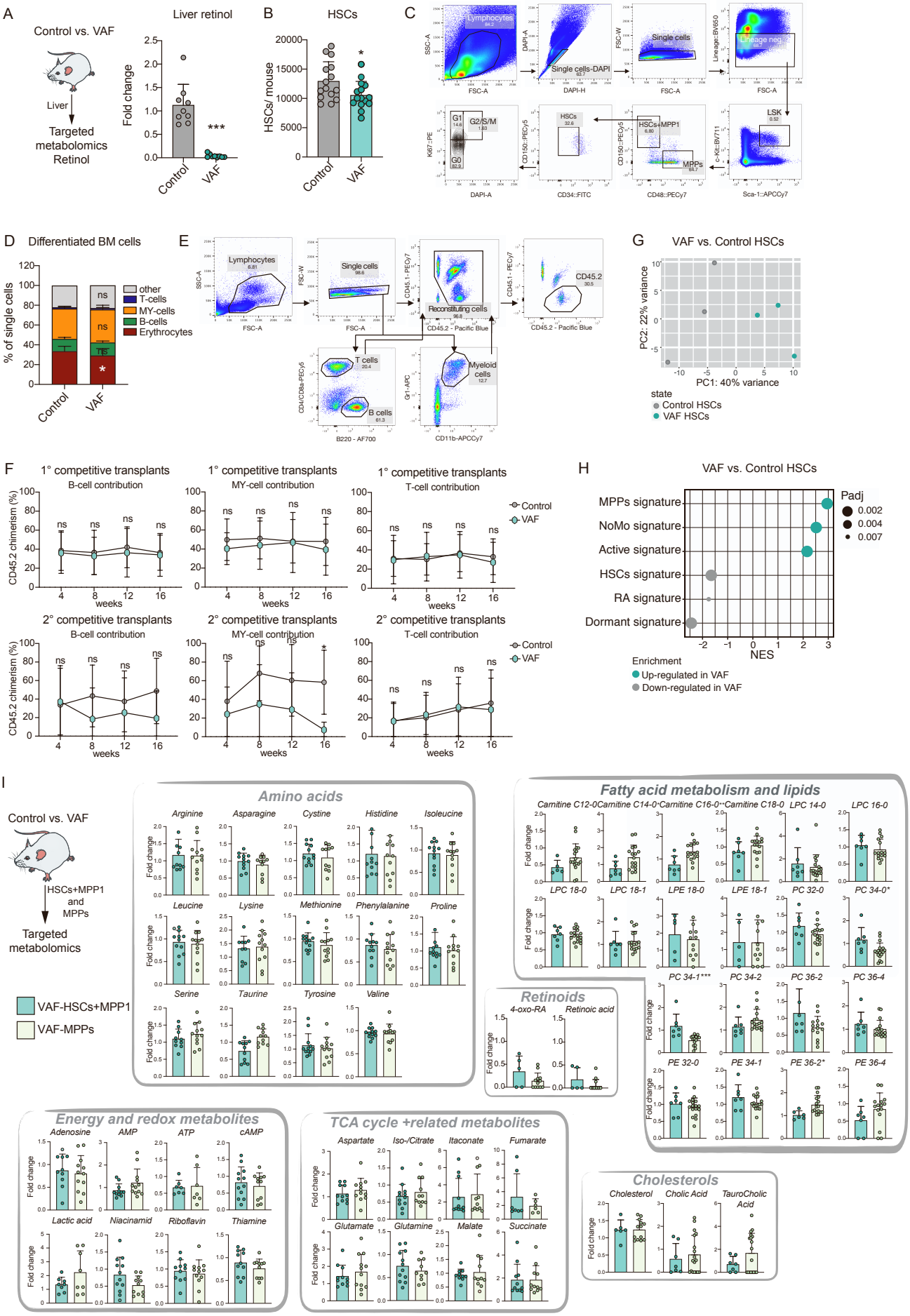

# Supplemental Figure 2

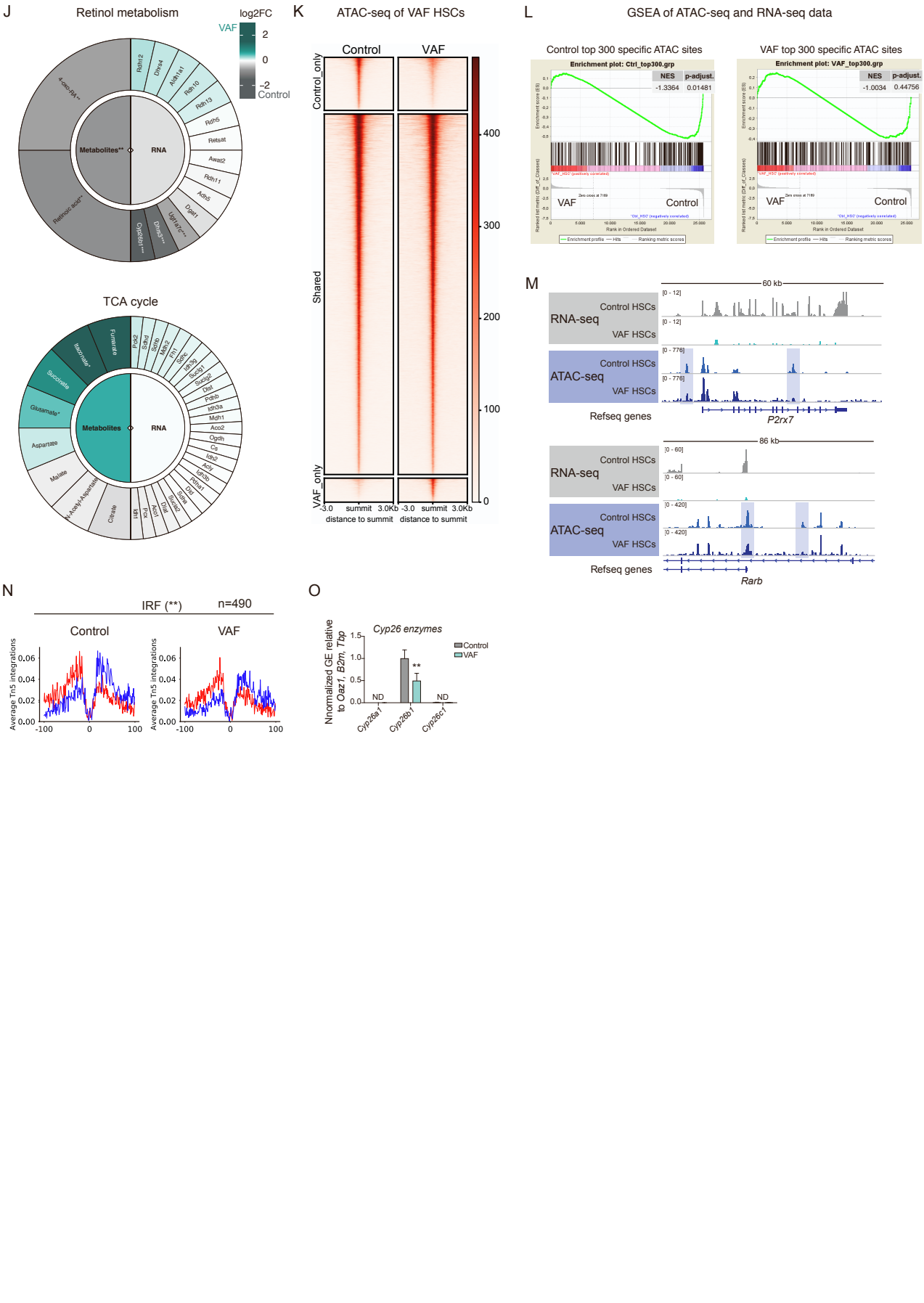

**Supplemental Figure 2 (related to Figure 2)**

**Lack of dietary vitamin A leads to loss of metabolic HSC identity and triggers differentiation**

(A) Targeted metabolomics results on liver of VAF and control diet. Depicted is fold change (FC) compared to control condition. n=9.

(B) Flow cytometric analysis of total HSC numbers in control and VAF. Cells per total mouse BM is shown. n=14-15.

(C) Representative gating scheme for flow cytometric analysis of cell cycle.

(D) Flow cytometric analysis of BM differentiated cell frequencies in control and VAF. Percentage of single cells is shown. n=12-15.

(E) Representative gating scheme for CD45.2 chimerism in PB.

(F) Flow cytometric analysis of CD45.2 PB chimerism of 1° and 2° competitive WBM transplantation assay of VAF and control conditions. Shown is B-cell, myeloid (MY)-cell and T-cell contribution over time as percentage of CD45.2 chimerism. n=9-16.

(G) PCA of RNA-seq data from VAF and control HSCs. Based on top 5,000 variable genes. n=3.

(H) RNA-seq data showing GSEA plots of published signatures in VAF vs. control HSCs.

(I) Schematic integration of targeted metabolomics results on VAF HSCs+MPP1 and VAF MPPs. Targeted metabolomics quantification depicted in bar diagrams. FC+SD relative to control-HSCs+MPP1. n=6-12.

(J) MTE-plots on the two KEGG pathways "retinol metabolism" and "TCA-cycle″. Depicted is log2FC between HSCs(+MPP1) in VAF and control; grey indicates up-regulated in control, green up-regulated in VAF. Significances calculated using an unpaired student’s t-test (metabolomics data set; *p <0.05; **p <0.01; ***p <0.001; ns, not significant) or by DESeq2 adjusted p-value (RNA-seq data set; *padj. <0.1; **p <0.05; ***p <0.01). Inner circles indicate the average tendencies of the entire KEGG pathway per data set; outer circles show individual genes/metabolites.

(K) ATAC-seq clustering on VAF and control HSCs. Heatmap of OCR peaks unique to control and VAF HSCs or shared. n=3.

(L) GSEA of top 300 ATAC-specific OCRs in HSCs vs. MPPs log2FC ranked RNA-seq comparison.

(M) Exemplary gene tracks on genes changing expression and chromatin accessibility in VAF HSCs compared to control.

(N) ATAC-seq digital footprinting analysis showing Tn5 insertions on forward and reverse strand (red, blue). IRF motif (half-site) in VAF and control HSCs.

(O) RT-qPCR validation of RNA-seq results on *Cyp26* enzymes gene expression in VAF and control HSCs. Normalized mean relative to *Oaz1, B2m,* and *Tbp* expression and relative to *Cyp26b1*. ND, not detected; GE, gene expression.

(A)-(B), (D), (F), (I), (O), mean +SD; (A)-(B), (I), (O), unpaired student's t-test. (D), and (F): two-way ANOVA. *p <0.05; **p <0.01; ***p <0.001; ns, not significant. Significance levels compared to control. n indicates number of biological replicates. For (A)-(B), (D), (F), (G), (I) and (O) two or more independent experiments were performed.

# Supplemental Figure 3

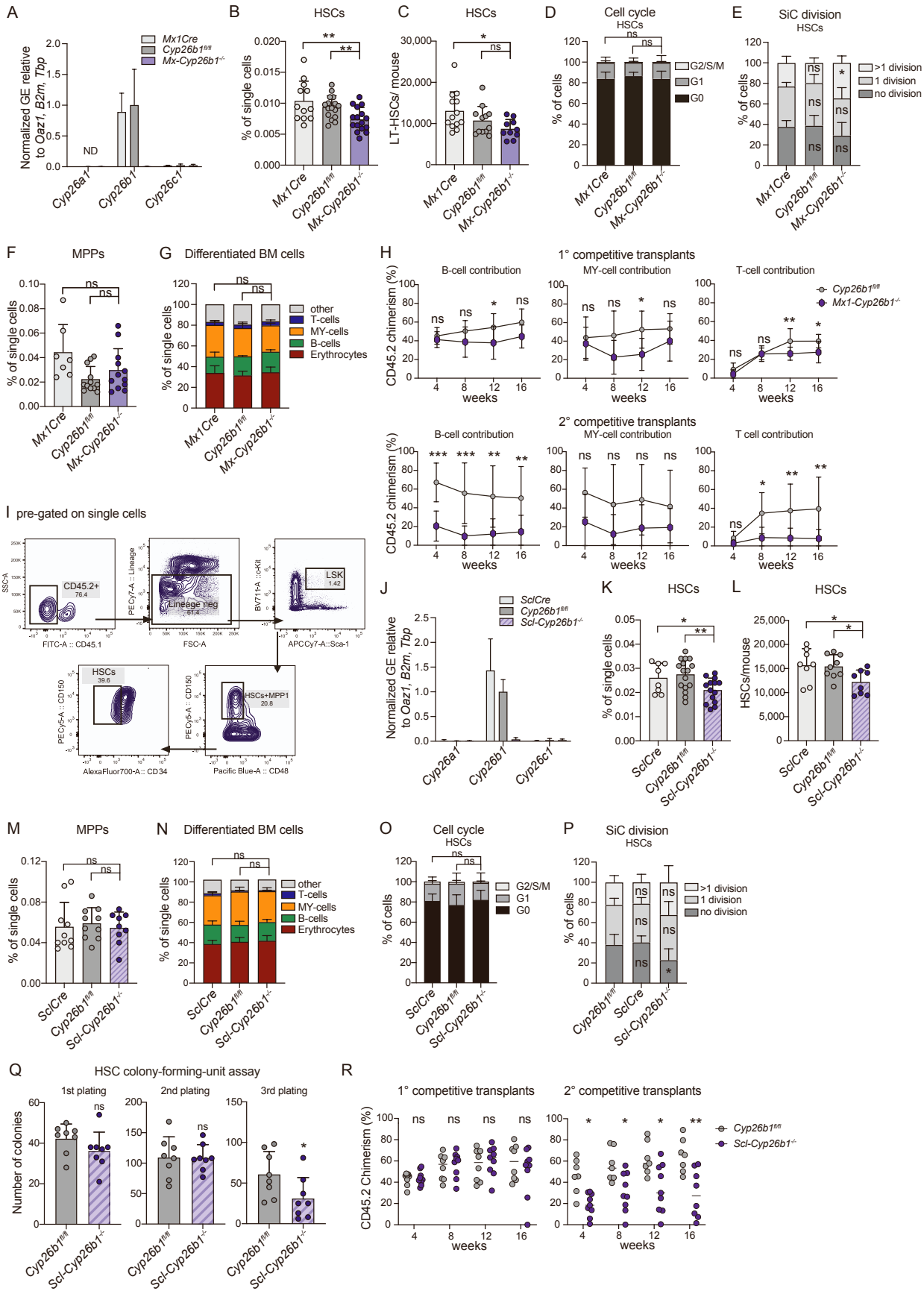

# Supplemental Figure 3

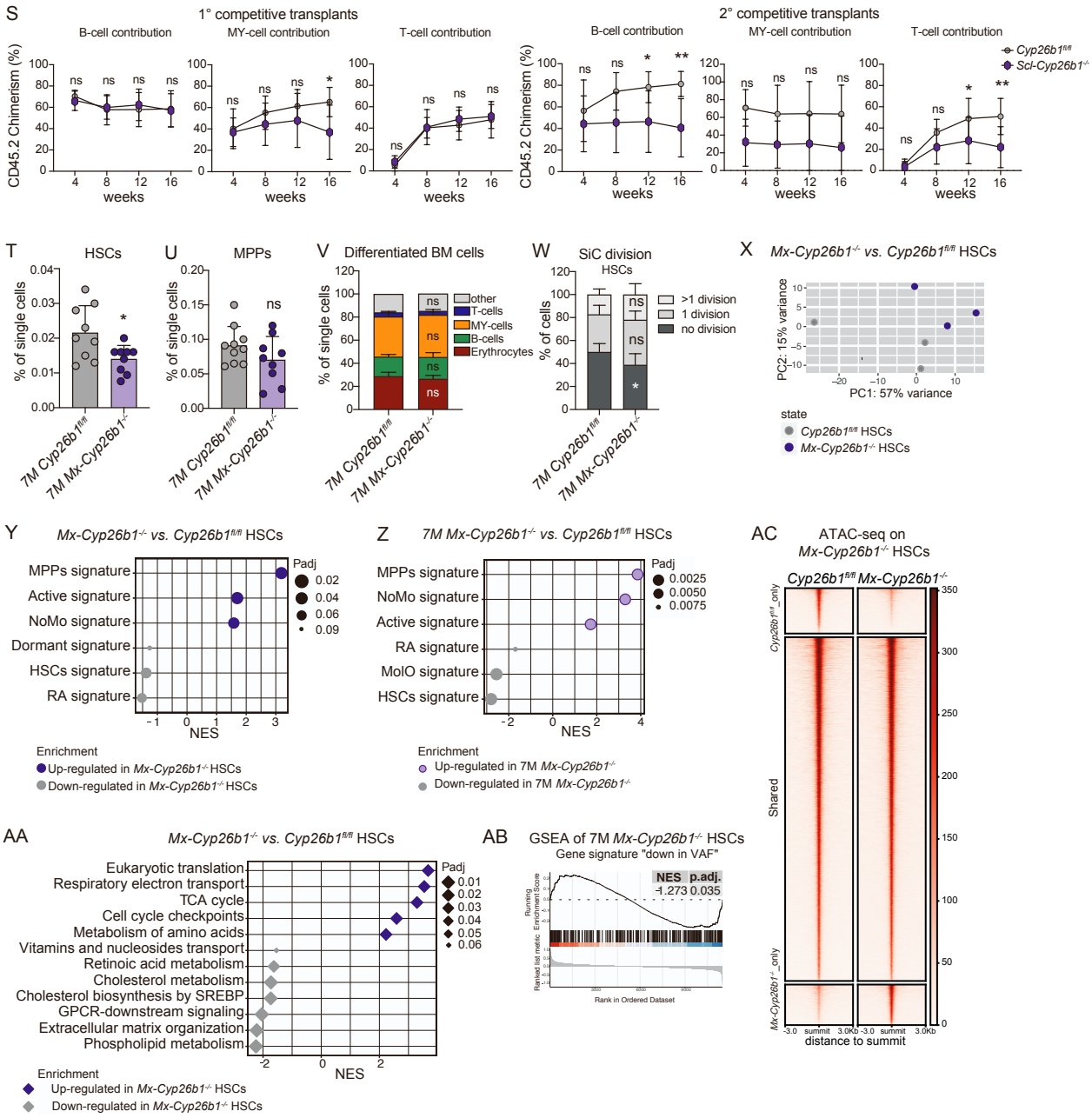

**Supplemental Figure 3 (related to Figure 3)**

**Cyp26b1 is critical for HSC self-renewal and quiescence**

(A) RT-qPCR analysis of *Cyp26 enzyme* gene expression in *Mx1Cre, Cyp26b1$^{fl/fl}$* (controls) and *Mx-Cyp26b1$^{-/-}$* (KO) HSCs. Normalized mean relative to *Oaz1, B2m,* and *Tbp* expression and relative to *Cyp26b1* in *Cyp26b1$^{fl/fl}$* HSCs is shown. ND, not detected; GE, gene expression.

(B) Flow cytometric analysis of HSC frequency in *Mx1Cre, Cyp26b1$^{fl/fl}$* and *Mx-Cyp26b1$^{-/-}$* mice. Percentage of single cells is shown. n=12-16.

(C) Flow cytometric analysis of HSC total numbers in *Mx1Cre, Cyp26b1$^{fl/fl}$* and *Mx-Cyp26b1$^{-/-}$*. Number of total HSCs per mouse BM is shown. n=10-13.

(D) Flow cytometric analysis of HSC cell cycle in *Mx1Cre, Cyp26b1$^{fl/fl}$* and *Mx-Cyp26b1$^{-/-}$*. Percentage of cell cycle phase (G0, G1, G2/S/M) is shown. n=16.

(E) Single cell (SiC) division assay of *Mx1Cre, Cyp26b1$^{fl/fl}$* and *Mx-Cyp26b1$^{-/-}$* HSCs. Frequency of cells is shown in percent. n=12.

(F) Flow cytometric analysis of MPPs frequencies in *Mx1Cre, Cyp26b1$^{fl/fl}$* and *Mx-Cyp26b1$^{-/-}$* mice. Percentage of single cells is shown. n=8-12.

(G) Flow cytometric analysis of differentiated BM cell frequencies in *Mx1Cre, Cyp26b1$^{fl/fl}$* and *Mx-Cyp26b1$^{-/-}$* mice. Percentage of single cells is shown. n=8-9.

(H) Flow cytometric analysis of CD45.2 PB chimerism of 1° and 2° competitive WBM transplantation assay of *Cyp26b1$^{fl/fl}$* and *Mx-Cyp26b1$^{-/-}$* conditions. Shown is B-cell, myeloid (MY) cell and T-cell contribution over time as percentage of CD45.2 chimerism. n=9-16.

(I) Representative gating scheme of flow cytometric analysis of BM CD45.2+ HSCs 16 weeks after transplantation.

(J) RT-qPCR analysis of *Cyp26b1* gene expression in *SclCre, Cyp26b1$^{fl/fl}$* (controls) and *Scl-Cyp26b1$^{-/-}$* (KO) HSCs. Normalized mean relative to *Oaz1, B2m, and Tbp* expression and relative to *Cyp26b1* in *Cyp26b1$^{fl/fl}$* HSCs is shown. GE, gene expression.

(K) Flow cytometric analysis of HSC frequency in *SclCre, Cyp26b1*$^{fl/fl}$ and *Scl-Cyp26b1*$^{-/-}$ mice. Percentage of single cells is shown. n=10.

(L) Flow cytometric analysis of HSC numbers in *SclCre, Cyp26b1*$^{fl/fl}$ and *Scl-Cyp26b1*$^{-/-}$mice. Absolute frequency of HSCs per mouse BM is shown. n=10.

(M) Flow cytometric analysis of MPPs frequency in *SclCre, Cyp26b1*$^{fl/fl}$ and *Scl-Cyp26b1*$^{-/-}$ mice. Percentage of single cells is shown. n=10.

(N) Flow cytometric analysis of BM differentiated cell frequency in *SclCre, Cyp26b1*$^{fl/fl}$ and *Scl-Cyp26b1*$^{-/-}$ mice. Percentage of single cells is shown. n=10.

(O) Flow cytometric analysis of cell cycle phase distribution in *SclCre, Cyp26b1*$^{fl/fl}$ and *Scl-Cyp26b1*$^{-/-}$ HSCs. Percentage of cells in cell cycle phase (G0, G1, G2/S/M) is shown. n=10.

(P) SiC division assay of *SclCre, Cyp26b1*$^{fl/fl}$ and *Scl-Cyp26b1*$^{-/-}$ HSCs. Frequency of cells is shown in percent. n=10-12.

(Q) Colony-forming unit (CFU) assay of *Cyp26b1*$^{fl/fl}$ and *Scl-Cyp26b1*$^{-/}$ HSCs. First, second and third plating. Colony numbers are normalized to control per plating. n=8.

(R) Flow cytometric analysis of CD45.2 PB chimerism of 1° and 2° competitive WBM transplantation assay of *Cyp26b1*$^{fl/fl}$ (CD45.2 control) and *Scl-Cyp26b1*$^{-/-}$ (CD45.2 KO) versus CD45.1/2 cells. Shown is the percentage CD45.2 chimerism over time. n=7-9.

(S) Flow cytometric analysis of CD45.2 PB chimerism of 1° and 2° competitive WBM transplantation assay of *Cyp26b1*$^{fl/fl}$ and *Scl-Cyp26b1*$^{-/-}$ conditions. Shown is B-cell, myeloid (MY) cell and T-cell contribution over time as percentage of CD45.2 chimerism. n=9-16.

(T) Flow cytometric analysis of HSC frequency in *Cyp26b1*$^{fl/fl}$ and *Mx-Cyp26b1*$^{-/-}$ 7-months (7M) after deletion of *Cyp26b1*. Percentage of single cells is shown. n=8-9.

(U) Flow cytometric analysis of MPP frequency in *Cyp26b1*$^{fl/fl}$ and *Mx-Cyp26b1*$^{-/-}$ 7M after deletion of *Cyp26b1*. Percentage of single cells is shown. n=9.

(V) Flow cytometric analysis of BM differentiated cell frequency in *Cyp26b1*$^{fl/fl}$ and *Mx-Cyp26b1*$^{-/-}$ 7M after deletion of *Cyp26b1*. Percentage of single cells is shown. n=9.

(W) SiC division assay of *Cyp26b1*$^{fl/fl}$ and *Mx-Cyp26b1*$^{-/-}$ HSCs 7M after deletion of *Cyp26b1*. Frequency of cells is shown in percent. n=9-12.

(X) PCA of RNA-seq data from *Mx-Cyp26b1*$^{-/-}$ compared to *Cyp26b1*$^{fl/fl}$ HSCs. Based on top 5,000 variable genes. n=3.

(Y) RNA-seq showing GSEA of published signatures in *Mx-Cyp26b1*$^{-/-}$ HSCs compared to *Cyp26b1*$^{fl/fl}$. n=3.

(Z) RNA-seq showing GSEA of published signatures in 7M *Mx-Cyp26b1*$^{-/-}$ HSCs compared to 7M *Cyp26b1*$^{fl/fl}$. n=2.

(AA) RNA-seq showing GSEA of selected Reactome pathways in *Mx-Cyp26b1*$^{-/-}$ compared to *Cyp26b1*$^{fl/fl}$ HSCs. n=3.

(AB) Gene set enrichment of down-regulated genes in VAF HSCs (padj.<0.1) in 7M *Mx-Cyp26b1*$^{-/-}$ versus 7M *Cyp26b1*$^{fl/fl}$ HSCs RNA-seq dataset.

(AC) Heatmap showing shared and specific OCRs in ATAC-seq on *Mx-Cyp26b1*$^{-/-}$ compared to *Cyp26b1*$^{fl/fl}$ HSCs. n=2.

(A)-(G), (J)-(W), mean +SD; (A)-(C), (F), (J)-(M), (Q), (T), unpaired student's t-test. (D)-(E), (G)-(H), (N)-(P), (R)-(S), (V), (W), two-way ANOVA. *p <0.05; **p <0.01; ***p <0.001. ns, not significant. n indicates number of biological replicates. Significance levels compared to control. For (A)-(H), (J)-(S) and (W)-(Z) two or more independent experiments were performed.

# Supplemental Figure 4

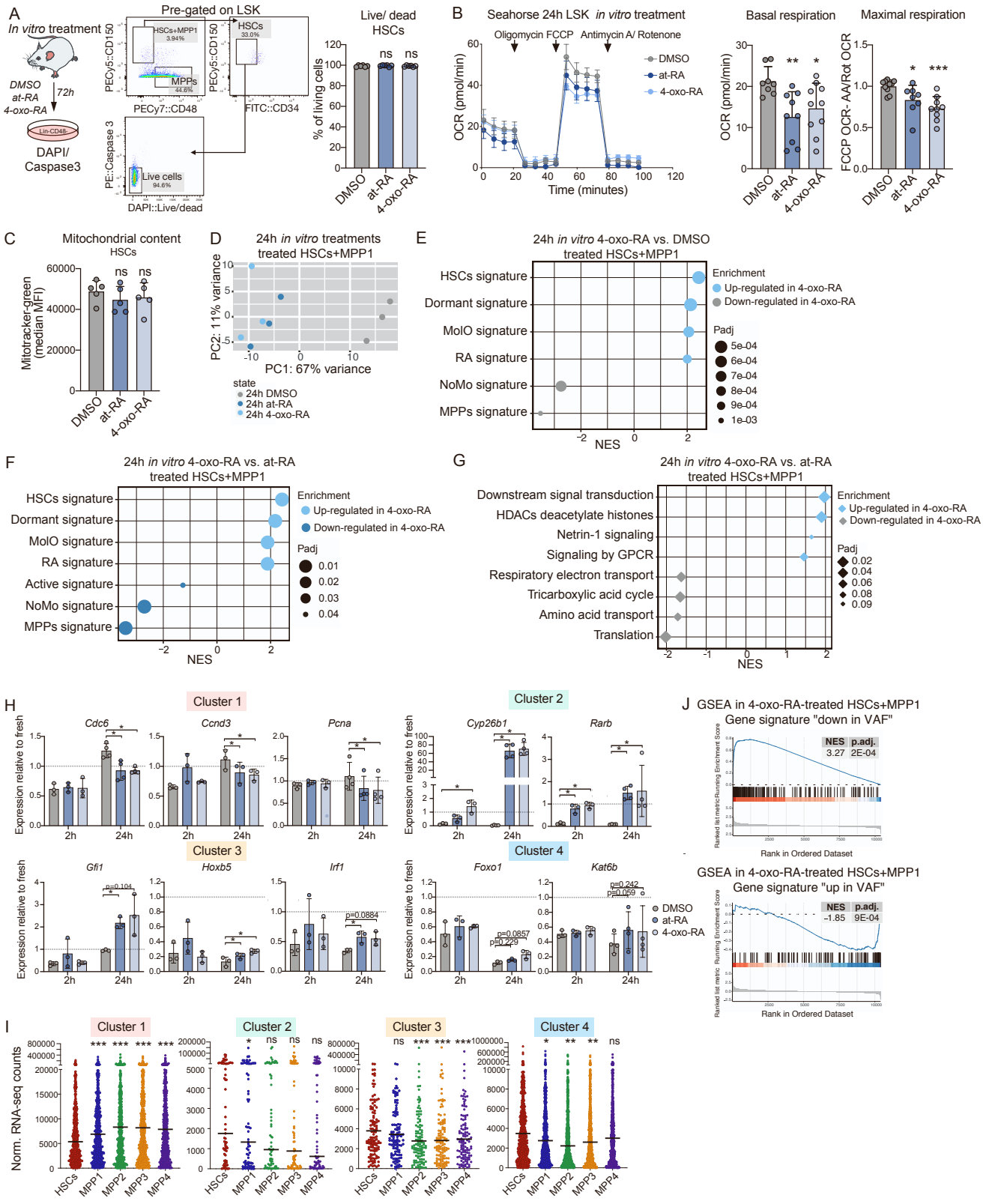

# Supplemental Figure 4

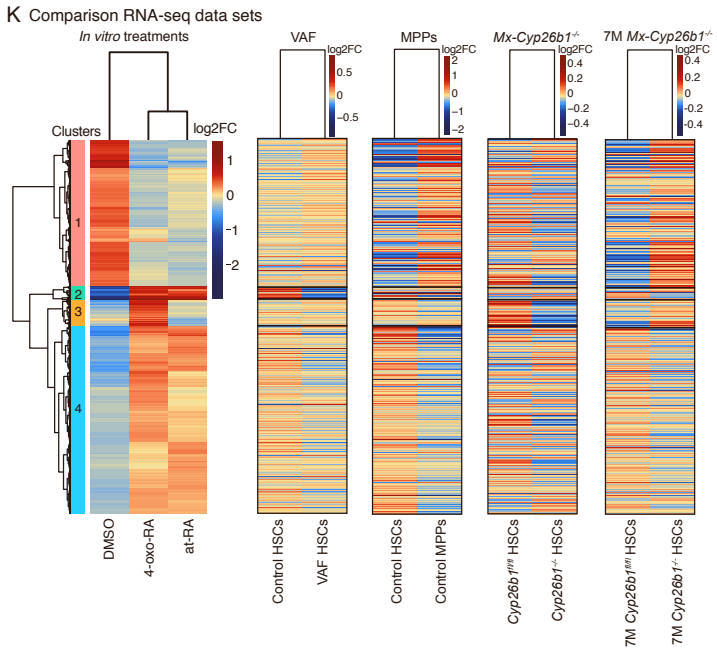

**Supplemental Figure 4 (related to Figure 4)**

**4-oxo-RA regulates HSC function**

(A) Representative gating scheme for live/dead cells after in *vitro treatments* of $Lin^-CD48^-$ cells with DMSO, at-RA and 4-oxo-RA. Flow cytometric analysis of HSCs. n=12.

(B) Seahorse assay after 72-h *in vitro* treatment of $5x10^5$ LSK cells with DMSO, at-RA and 4-oxo-RA. Representative Seahorse assay showing oxidative consumption rate (OCR) in pmol/min over time after Oligomycine, FCCP and Antimycine A + Rotenone injection. Basal respiration is shown in pmol/min. Maximal respiration is normalized to DMSO. n=8-10. (C) Flow cytometric analysis of mitochondrial content after 24-h *in vitro* treatments of $Lin^-CD48^-$ cells with DMSO, at-RA, and 4-oxo-RA. Shown is median fluorescence intensity (MFI) of Mitotracker green. Gated on HSCs. n=5.

(D) PCA of 24-h *in vitro* treatment RNA-seq data. Based on top 5,000 variable genes. n=3.

(E) RNA-seq data showing GSEA of published signatures comparing 4-oxo-RA and DMSO conditions of 24-h *in vitro* treatment HSCs+MPP1.

(F) RNA-seq data showing GSEA of published signatures comparing 4-oxo-RA and at-RA conditions of 24-h *in vitro* treatment HSCs+MPP1.

(G) RNA-seq data showing GSEA of selected "Reactome pathways" comparing 4-oxo-RA and at-RA conditions of 24-h *in vitro* treatment HSCs+MPP1.

(H) RT-qPCR of gene expression of *in vitro*-treated HSCs+MPP1. Validation of RNA-seq results for *in vitro* treatments (24h). Depicted is gene expression after 2-h and 24-h DMSO, at-RA, and 4-oxo-RA treatment is depicted. Normalized to mean of fresh (0-h) HSCs+MPP1 relative to *Oaz1* expression. n=3-4.

(I) Gene expression over the course of differentiation. Depicted is the median of RNA-seq read counts in HSCs and MPP1/2/3/4, respectively (data published in Cabezas-Wallscheid et al., 2014) for all genes associated in each cluster (*in vitro* treatments RNA-seq heatmap). Normalized RNA-seq read counts are shown.

(J) RNA-seq showing gene set enrichment of up- and down-regulated genes in VAF HSCs (padj.<0.1) in 4-oxo-RA versus DMSO *in vitro*-treated HSCs+MPP1.

(K) Heatmap of RNA-seq data of 24-h *in vitro*-treated HSCs+MPP1. Unbiased clustering identified 4 main clusters. Comparison to RNA-seq normalized counts heatmap in VAF HSCs, MPPs, *Mx-Cyp26b1*$^{-/-}$ HSCs and 7 months (7M) *Mx-Cyp26b1*$^{-/-}$ HSCs.

(A)-(C), (H): mean +SD, (A), (C), (H), unpaired student's t-test. *p <0.05; **p <0.01; ***p <0.001; ns, not significant. n indicates number of biological replicates. Significance levels compared to control. For (A)-(C), and (H) two or more independent experiments were performed.

# Supplemental Figure 5

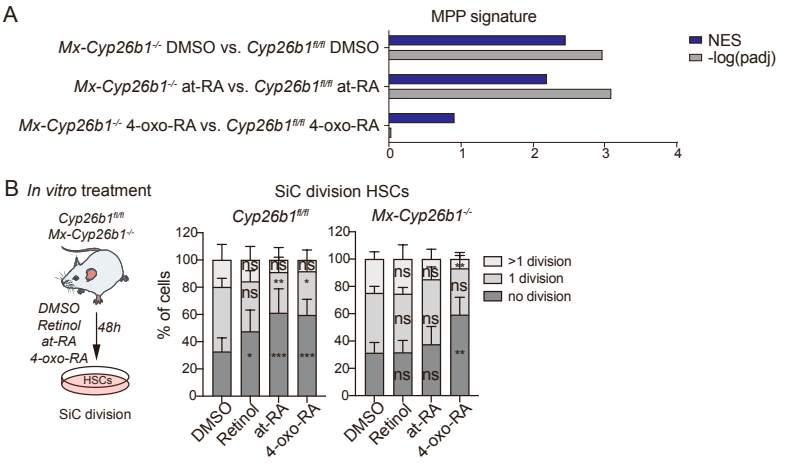

**Supplemental Figure 5 (related to Figure 5)**

**The Cyp26b1 downstream metabolite 4-oxo-RA is required for HSC maintenance**

(A) RNA-seq data showing GSEA of published MPP signature (Cabezas Wallscheid et al., 2014) comparing *Cyp26b1*$^{fl/fl}$ and *Mx-Cyp26b1*$^{-/-}$ HSCs+MPP1 for each 24h *in vitro* treatment DMSO, at-RA, and 4-oxo-RA, respectively. Normalized enrichment score (NES) and -log(padj.) are shown.

(B) Workflow showing single cell (SiC) division assay after *in vitro* treatment of *Mx-Cyp26b1*$^{-/-}$ compared to *Cyp26b1*$^{fl/fl}$ with DMSO, retinol, at-RA, and 4-oxo-RA. SiC division assay of treated HSCs. Percentage of single cells is shown. n=12. Two-way ANOVA performed. *p <0.05; **p <0.01; ***p <0.001; ns, not significant.

# Supplemental Figure 6

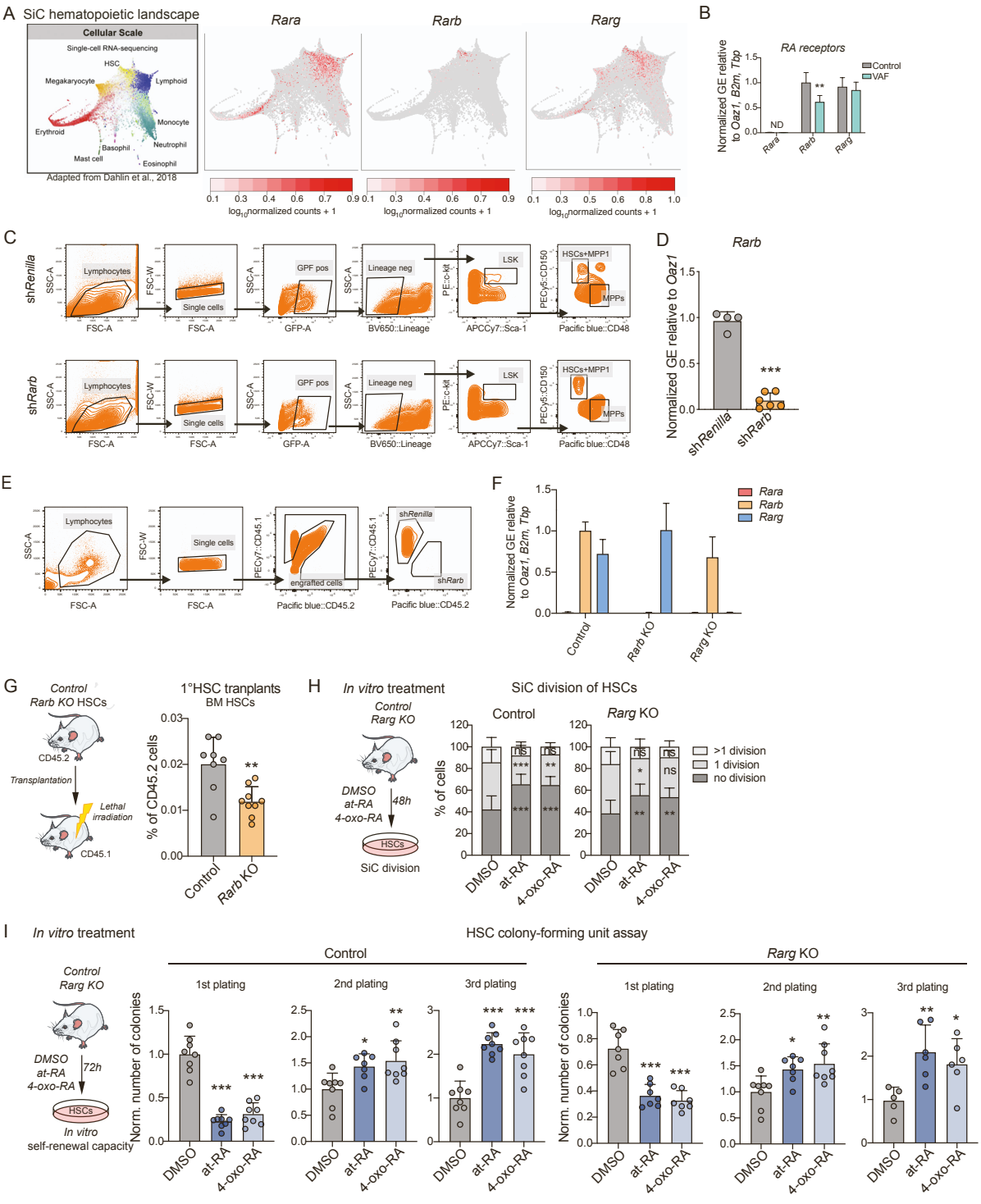

**Supplemental Figure 6 (related to Figure 6)**

**Rarb is required to mediate 4-oxo-RA-dependent maintenance of HSC self-renewal**

(A) Single cell data set from Dahlin et al. 2018, published in Blood (Dahlin et al., 2018). Expression of RA receptors within a $Lin^-$ $c\text{-}Kit^+$ compartment.

(B) RT-qPCR validation of RNA-seq results on *RAR* gene expression in VAF and control HSCs. Normalized mean relative to *Oaz1, B2m and Tbp* expression and relative to *Rarb*. ND, not detected; GE, gene expression

(C) Representative gating scheme after transfection.

(D) RT-qPCR analysis of *Rarb* gene expression after *in vitro Rar*b knock-down with sh *Renilla* (control) and sh*Rarb*. Normalized mean expression relative to *Oaz1* is shown. n=4-6. GE, gene expression.

(E) Representative gating scheme for CD45.2 chimerism of *Rar*b KD transplantation.

(F) RT-qPCR analysis of *Rara, Rarb* and *Rarg* gene expression in *Rarb* KO and *Rarg* KO HSCs compared to control. Normalized mean relative to *Oaz1, B2m,* and *Tbp* expression and relative to *Rarb* expression in control HSCs is shown. n=6. GE, gene expression.

(G) Flow cytometric analysis of $CD45.2^+$ HSCs 16 weeks after 1° transplantation of HSCs derived from *Rarb* KO mice. Percentage of CD45.2 cells is shown. n=8-9.

(H) Workflow showing single cell (SiC) division assay after *in vitro* treatment of control compared to *Rarg* KO with DMSO, at-RA and 4-oxo-RA. SiC division assay of treated HSCs. Percentage of single cells is shown. n=9.

(I) Workflow depicting colony-forming unit (CFU) assay after *in vitro* treatment of control compared to *Rarg* KO with DMSO, at-RA and 4-oxo-RA. CFU assay after 72h of treated HSCs. Number of colonies normalized to control DMSO treatment of each corresponding plating. n=5-8.

Panels (B), (D), (F)-(I), mean +SD; (B), (D), (F)-(G), (I), unpaired student's t-test; (H), two-way ANOVA. *p <0.05; **p <0.01; ***p <0.001. ns, not significant. n indicates number of biological replicates. Significance levels compared to control. For (B) and (D)-(G), two or more independent experiments were performed.